# A Monte Carlo-Based Probabilistic Approach to Switching Loss Estimation in Power MOSFETs

**Wesley J. de Paula**⊚[1,*], **Guilherme M. Soares**⊚[2], **Pedro S. Almeida**⊚[2],
**Henrique A. C. Braga**⊚[2]

[1]Federal University of São João del-Rei, Department of Telecommunications Engineering and Mechatronics, Ouro Branco, MG, Brazil.
[2]Federal University of Juiz de Fora, Department of Electrical Engineering, Juiz de Fora, MG, Brazil.

e-mail: wesleyjosias@ufsj.edu.br[*]; guilherme.marcio@ufjf.br; pedro.almeida@ufjf.br; henrique.braga@ufjf.br.
[*]Corresponding author.

**ABSTRACT** Switching losses have been shown to have a significant impact on the efficiency and thermal management of power electronic systems, particularly in high-performance converters. Conventional estimation techniques frequently rely on deterministic parameters, which are unable to account for the inherent variability in semiconductor characteristics and gate-driving conditions. This limitation can result in erroneous predictions and an underestimation of design margins. In order to address this issue, the present paper proposes a probabilistic approach for estimating switching losses in MOSFETs, with applications demonstrated for both Silicon carbide (SiC) and Silicon (Si) devices, using the Monte Carlo method. The methodology involves treating key device and driver parameters, such as gate resistance, transconductance, and threshold voltage, as statistical variables. This approach enables the capture of inherent uncertainties in device behavior. The switching transients are characterized through Double Pulse Test (DPT) simulations across a wide range of voltage and current levels. Monte Carlo simulations are extensively performed to derive the statistical distribution of energy losses, ensuring realistic performance expectations under variable conditions. The findings indicate that parameter variability can lead to substantial discrepancies in switching loss predictions, underscoring the limitations of conventional deterministic methods. The proposed methodology provides a more robust and reliable foundation for thermal design, loss prediction, and reliability assessment in power converter applications, ultimately ensuring improved performance and increased lifespan of power electronic systems.

**KEYWORDS** Monte Carlo Simulation, Silicon Carbide MOSFET, Statistical Analysis, Switching Losses, Parameter Variability.

## I. INTRODUCTION

Modern power electronics systems necessitate semiconductor devices capable of functioning at elevated voltages, temperatures, and switching frequencies while sustaining high conversion efficiency. These requirements are of particular importance in the domains of automotive electrification, renewable energy integration, and industrial power conversion systems [1], [2]. Silicon carbide power MOSFETs have emerged as an innovative solution, overcoming the fundamental limitations of silicon-based power devices through their superior material properties, including a wide bandgap $> 3$ eV and high critical electric field strength 2-3 MV/cm [3].

The performance advantages of SiC MOSFETs become especially significant as power electronic systems evolve toward higher switching frequencies, where conventional silicon devices exhibit substantial switching losses. These losses have consequences for the overall efficiency of the system. In addition, they impose limitations on power density by necessitating the use of larger thermal management solutions [4].

A significant challenge in system design resides in the development of practical yet accurate methods for predicting MOSFET switching losses through the utilization of solely commercially available datasheet parameters. These methodologies enable engineers to reliably estimate junction temperatures and converter efficiency early in the design phase, a critical consideration in applications such as electric vehicle drivetrains and grid-tied inverters, where operational reliability is paramount. Despite these advances, proper characterization of their switching behavior remains essential for real-world applications [5]. In high-performance converters, switching losses frequently dominate conduction losses, particularly as switching frequencies increase to achieve higher power density [6], [7]. However, while conduction losses are relatively straightforward to calculate, switching losses are more challenging due to the lack of detailed data in MOSFET datasheets, especially across all operating conditions. These losses emerge from the overlap of the drain-to-source voltage ($v_{DS}$) and drain current ($i_D$) during switching transitions, and their accurate estimation

requires precise characterization of the voltage and current waveforms, including their rise and fall times.

Despite extensive research on power loss estimation, a reliable method for accurately predicting switching losses is still lacking in power electronics [8]–[11]. Variations in key parameters, such as gate resistance, transconductance, and threshold voltage, have a significant impact on switching losses, yet they are often neglected in conventional estimation models [12] [13].

Furthermore, most commercial datasheets do not provide sufficient data to capture these variations across different operating conditions, presenting a challenge for a more general estimation. As such, there remains a gap in the literature regarding the development of more accurate models that account for these variations, particularly in the context of real-world operating conditions.

Monte Carlo simulations have been extensively used to model stochastic behavior in power electronics, particularly in reliability assessments and loss estimations [14], [15]. Previous research has applied this technique to various applications, such as photovoltaic inverters and wind turbine power converters [16], [17]. These methods allow the incorporation of parameter uncertainty and process tolerances into prediction models, improving the statistical reliability of the simulation outcomes. However, existing studies often lack a systematic treatment of how variations in key switching parameters influence loss predictions, especially under dynamic thermal and electrical stress conditions.

This paper aims to address this gap by proposing a probabilistic approach for estimating switching losses in Si and SIC MOSFETs, incorporating the inherent variability in device parameters. The proposed approach utilizes Monte Carlo simulations to model the uncertainty in these parameters, providing a more accurate and realistic prediction of switching losses, which is crucial for optimizing thermal management and improving overall system efficiency.

The structure of this paper is organized as follows: Section II discusses the evaluation of hard-switching transients and the impact of parametric variations. Section III provides an overview of the Monte Carlo method. Section IV details the implementation of the probabilistic estimation approach. Section V presents experimental results and discussion. Finally, Section VI concludes the paper.

## II. EVALUATION OF HARD-SWITCHING TRANSIENTS IN POWER MOSFETS

### A. Hard-switching Phenomena

To analyze hard-switching conditions, the double-pulse test circuit illustrated in Figure 1 is widely recognized as the standard method for characterizing the switching behavior of MOSFETs and IGBTs. The gate–drain capacitance ($C_{gd}$), gate–source capacitance ($C_{gs}$), and drain–source capacitance ($C_{ds}$) are considered, along with the gate driver output voltage ($V_{dr}$), gate resistance ($R_g$) comprises both the internal and external resistances connected in series, and the DC-
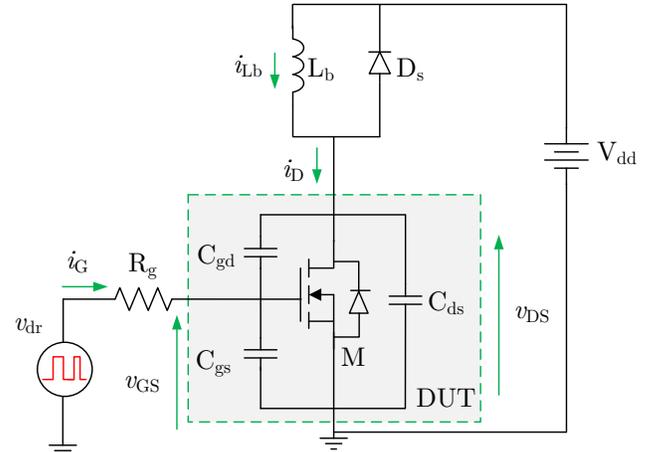


**FIGURE 1. Diagram of the double-pulse test circuit, a common experimental setup for evaluating the switching losses of a MOSFET (M) or DUT.**

bus voltage ($V_{dd}$). Additionally, an auxiliary branch composed of an inductor ($L_b$) in parallel with a diode ($D_s$) is incorporated to facilitate both the analytical framework and the measurement procedures. Figure 2 illustrates the idealized switching process. This setup is widely adopted by semiconductor manufacturers as it effectively reproduces the operating conditions of conventional PWM hard-switching converters under inductive load, which is typical in most power electronic systems.

By examining both turn-on and turn-off transitions, this test enables a comprehensive assessment of the transient behavior of power devices under various operating conditions. Moreover, it facilitates the evaluation of MOSFET performance across different current levels and input voltages while ensuring that the device's junction temperature remains relatively stable.

Based on the waveforms presented in Figure 2, it is possible to derive the equations that describe the complete switching process. These expressions are adapted from the methodology proposed by Brown [18]. The switching behavior of the MOSFET can be segmented into six distinct
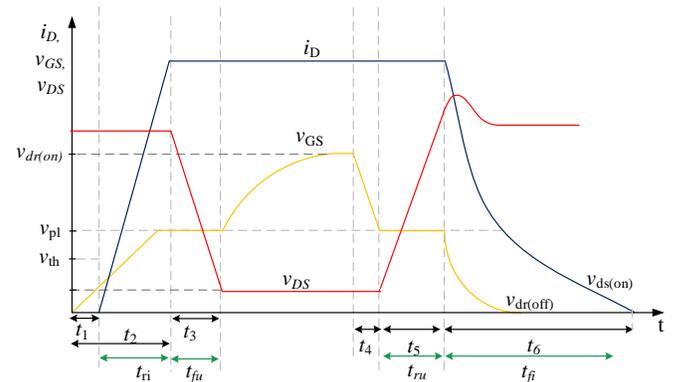


**FIGURE 2. Typical MOSFET switching waveforms. Adapted from [18].**

intervals, each corresponding to a different phase of the transition. The expressions corresponding to time intervals $t_1$, $t_2$, and $t_3$ during the turn-on transient are provided in (1), (2), and (3), respectively.

$$t_1 = R_g \cdot (C_{gs} + C_{gd}) \cdot \ln\left(\frac{v_{dr(on)}}{v_{dr(on)} - V_{th}}\right) \qquad (1)$$

where $v_{dr(on)}$ represents the high-level output voltage applied to the external gate resistance; $V_{th}$ is defined as the gate voltage at which the device starts to turn-on.

$$t_2 = R_g \cdot (C_{gs} + C_{gd}) \cdot \ln\left(\frac{v_{dr(on)}}{v_{dr(on)} - v_{pl}}\right) \qquad (2)$$

According to Figure 2, $t_3$ represents the voltage fall time to the on-state level during turn-on ($t_{fu}$), while the rise time of the current ($t_{ri}$) is given by the duration between $t_1$ and $t_2$.

In practice, the drain–source capacitance ($C_{ds}$) of a given MOSFET is influenced by at least two distinct factors. The first is the drain–source voltage ($v_{DS}$), which directly affects the junction capacitance. As $v_{DS}$ increases, $C_{ds}$ decreases significantly due to the widening of the depletion region, a well-known nonlinear behavior extensively documented in the literature for both Si and SiC devices [19]. Notably, the majority of these studies have focused on operating conditions characterized by a zero or negative gate–source voltage ($v_{gs}$), under which the MOSFET is ensured to remain in the fully off-state.

Nevertheless, during the ON-state or the switching transitions, $C_{ds}$ is also affected by the presence of the conductive channel and the nonuniform electron distribution induced by the gate–drain potential difference. This represents the second influencing factor, which, to the best of the authors' knowledge, has received limited attention in the literature for both Si and SiC MOSFETs.

It is important to highlight that this effect is more pronounced in SiC MOSFETs when compared to their Si counterparts with similar power ratings. This is primarily due to the higher gate-drive voltages and lower on-state resistance of SiC devices, which, combined with their faster switching capabilities, enhance the impact of this phenomenon on transient simulation accuracy.

Given the aforementioned considerations regarding the variation of $C_{rss}$ and its influence on the switching behavior, a more accurate modeling approach becomes necessary. In this context, the proposed method incorporates the voltage-dependent nature of the reverse transfer capacitance ($C_{rss}$), as previously illustrated in Figure 3.

In light of these aspects and the associated variation of the gate–source capacitance ($C_{gs}$) during switching events, an enhanced modeling strategy is employed to improve the accuracy of the transient characterization. This approach allows for a better representation of the dynamic behavior of the device, particularly under high-speed switching conditions.
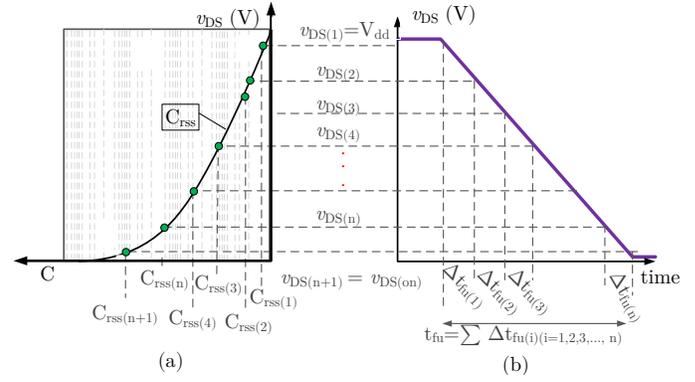


FIGURE 3. (a) Generic parasitic capacitance waveforms of a MOSFET and (b) drain-to-source voltage variation during switching transitions.

The proposed implementation methodology consists of determining the specific capacitances based on the drain-to-source voltage corresponding to different subintervals of the switching process. In this approach, a set of voltages ranging from $V_{dd}$ to $V_{ds(on)}$ is defined according to the specific capacitance $C_{rss}$. In Figure 3(b), each time segment is associated with the voltage fall time $\Delta t_{fu}(i)$. It is assumed that these subintervals are sufficiently small, ensuring that $C_{rss}$ remains approximately constant within each interval. Consequently, the total voltage fall time $t_{fu}$ is obtained by summing all subintervals $\Delta t_{fu}(i)$.

To provide a clearer explanation of the method, the voltage fall time is divided into $n$ subintervals, requiring $n+1$ discrete voltage levels $v_{DS}$. The total transition time $t_{fu}$ is then given by (3).

$$t_3 = t_{fu} = \sum_{i=1}^{n} R_g \cdot C_{rss(i+1)} \frac{v_{DS(i+1)} - v_{DS(i)}}{v_{dr(on)} - v_{pl}}. \qquad (3)$$

Similarly, the voltage rise time is obtained using (4):

$$t_5 = t_{ru} = \sum_{i=1}^{n} R_g \cdot C_{rss(i+1)} \frac{v_{DS(i+1)} - v_{DS(i)}}{v_{pl} - v_{dr(off)}}. \qquad (4)$$

where $i = 1, 2, 3, \ldots, n$.

The time intervals associated with the current during the turn-on and turn-off phases of the MOSFET are determined by (5) and (6), respectively.

$$t_{ri} = R_g \cdot C_{iss} \cdot \ln\left(\frac{g_{fs} \cdot (v_{dr(on)} - V_{th})}{g_{fs} \cdot (v_{dr(on)} - V_{th}) - i_D}\right) \qquad (5)$$

$$t_{fi} = R_g \cdot C_{iss} \cdot \ln\left(\frac{v_{th} + \frac{i_D}{g_{fs}}}{v_{th}}\right), \qquad (6)$$

Additionally, the energy losses can be computed using (7), (8), and (9), allowing for the quantification of switching losses in the device.

The switching energy during turn-on ($E_{on}$) is given by:

$$E_{on} = E_{t_{ri}} + E_{t_{fu}} = \frac{1}{2} \cdot v_{DS} \cdot i_D (t_{ri} + t_{fu}), \qquad (7)$$

The switching energy during turn-off ($E_{off}$) is given by:

$$E_{off} = E_{t_{ru}} + E_{tf_i} = \frac{1}{2} v_{DS} \cdot i_D \left( t_{ru} + t_{fi} \right), \quad (8)$$

The total switching energy ($E_{sw}$) is the sum of the turn-on and turn-off energies:

$$E_{sw} = \frac{1}{2} \cdot v_{DS} \cdot i_D \left( t_{ri} + t_{fu} + t_{ru} + t_{fi} \right). \quad (9)$$

The switching loss estimation method was implemented based on the flowchart shown in Figure 4. Each step corresponds to a specific stage in the algorithm:

1) System specifications are loaded, including device parameters and operating conditions.
2) The $v_{DS}$ vector is defined, ranging from $V_{ds(on)}$ to $V_{dd}$, with a given step size $V_{step}$.
3) The iteration index is initialized to $i = 1$.
4) For each voltage level in the $v_{DS}$ vector:
   a) Check whether $i > 0$ to determine if there are levels to process.
   b) Compute the capacitance $C_{rss}$ as a function of the input voltage.
   c) Determine the switching intervals $t_{fu}$ and $t_{ru}$.
   d) Increment the index $i = i + 1$ and repeat the loop until all levels are covered.
5) Compute the switching transition times $t_{ri}$ and $t_{fi}$ using (5) and (6).
6) Estimate the energy losses $E_{on}$, $E_{off}$, and total switching energy $E_{sw}$ using (7)–(9)
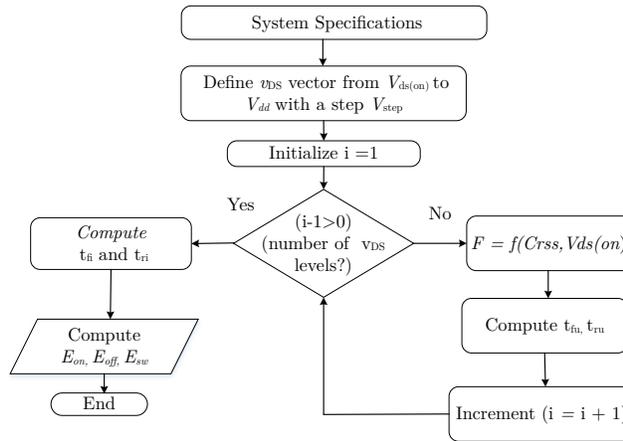


FIGURE 4. Flowchart for switching loss calculation.

During intervals where the drain–source voltage undergoes rapid transitions (i.e., high $dv/dt$ events), the intrinsic capacitances are treated as nonlinear, bias-dependent quantities. To capture this behavior, the switching transition is discretized into small subintervals, and the capacitance values are updated at each step based on curves obtained from the datasheet. The reverse transfer capacitance $C_{rss}$ (associated with $C_{gd}$ is interpolated as a function of the instantaneous $v_{DS}$, while the input capacitance $C_{iss}$ is used to determine the effective $C_{gs}$. These discretized values are then employed in the computation of the switching intervals and the corresponding energy losses ($E_{on}$, $E_{off}$, $E_{sw}$), ensuring that the nonlinear effects of the device capacitances are properly reflected in the energy estimation.

### B. Impact of Parametric variations

This subsection presents a relative sensitivity analysis aiming to quantify the effect of variations in key input parameters on the estimated switching losses.

The analytical method typically exhibits relative errors under specific operating conditions. These inaccuracies are primarily attributed to uncertainties and imprecisions in the input parameters commonly extracted from manufacturer datasheets. Therefore, assessing the influence of these parameters on the results generated by switching loss estimation models is essential to validate the reliability and accuracy of such predictions.

The considered parameter variations are constrained within realistic bounds, as commonly encountered in practical applications. To illustrate the methodology, the SiC MOSFET SCT3120AL [20] is used as the reference device throughout this study.

The main evaluated parameters and their respective variation ranges are summarized in Table 1. As shown, the values for transconductance, threshold voltage, and external gate resistance are obtained from the device datasheet.

In this work, the threshold voltage ($V_{th}$) and transconductance ($g_{fs}$) are treated as independent parameters. This assumption was adopted as a practical alternative because $g_{fs}$ depends on physical quantities such as mobility, oxide capacitance, and device geometry, which are not fully specified in manufacturer datasheets. The datasheet-provided ranges and/or curves were used to represent parameter variability, allowing the Monte Carlo methodology to account for device parameter spread while maintaining a feasible and reproducible simulation procedure. Although $V_{th}$ and $g_{fs}$ are physically correlated, this correlation is not explicitly modeled here. Nevertheless, the accuracy of the proposed approach has been verified through experimental validation, demonstrating that this simplification does not compromise the reliability of the results.

TABLE 1. Evaluated parameters of the SiC MOSFET SCT3120AL

| MOSFET | Range of the evaluated parameters | | |
|---|---|---|---|
| | $g_{fs}$ [S] | $V_{th}$ [V] | $R_{g(\text{ext})}$ [Ω] |
| SCT3120AL | 0.5 – 5.6 | 2.7 – 5.6 | 10 – 15 |
| Base Value | 2.7 | 4.15 | 10 |

Each input parameter is normalized with respect to its base value using the expression:

$$\overline{X}_{\text{norm}} = \frac{X}{X_b} \tag{10}$$

where $X$ denotes the evaluated parameter, $X_b$ represents its base value, and $\overline{X}_{\text{norm}}$ is the corresponding normalized value.

The sensitivity analysis quantifies the impact that uncertainties in the MOSFET's input parameters have on the estimated switching losses, $E_{sw}$. The sensitivity of a given parameter, denoted as $X_{\text{sens}}$, is computed using the following expression:

$$X_{\text{sens}} = \frac{(E_{\max} - E_{\min})/E_{\text{base}}}{\overline{X}_{\text{norm(max)}} - \overline{X}_{\text{norm(min)}}} \tag{11}$$

where $E_{\max}$ and $E_{\min}$ are the maximum and minimum switching energy values observed within the parameter variation range, $\overline{X}_{\text{norm(max)}}$ and $\overline{X}_{\text{norm(min)}}$ are the corresponding normalized extremes of the evaluated parameter, and $E_{\text{base}}$ is the energy value associated with the base parameter. Since the switching energies are normalized with respect to $E_{\text{base}}$, the resulting sensitivity $X_{\text{sens}}$ is a dimensionless quantity.

Figure 5 reveals that the most influential parameters are the threshold voltage ($V_{th,\text{sens}} = 0.49$) and the external gate resistance ($R_{g,\text{sens}} = 0.75$), while the transconductance exhibits a considerably lower sensitivity of 0.03. Similar trends were observed under different voltage and current conditions, suggesting the robustness of the proposed analysis.
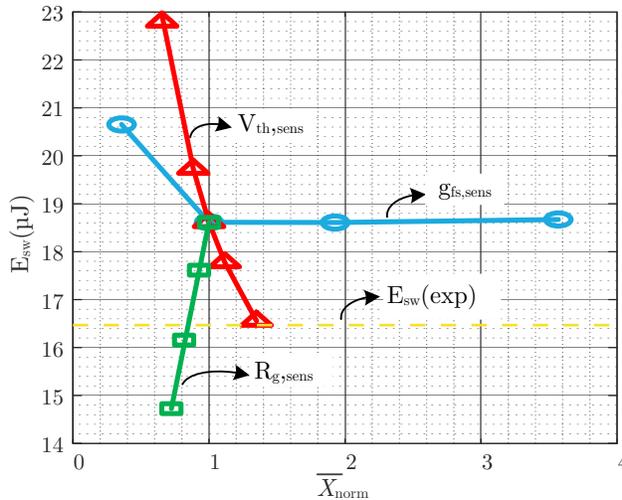


**FIGURE 5. Normalized sensitivity analysis of switching losses as a function of parameter variations.**

## III. OVERVIEW OF THE MONTE CARLO METHOD

The Monte Carlo Method (MCM) provides approximate solutions to various mathematical problems through statistical sampling performed by a computer using random or pseudo-random number generators, which constitute the core of the method [21]. This approach is particularly applicable to both deterministic problems and inherently stochastic ones.

One of the main advantages of MCMs is the elimination of the need to derive complex differential equations describing system behavior. Instead, the system is represented through probability density functions (PDFs), allowing random sampling based on these distributions. This process is iteratively executed, and the desired outcome is obtained using statistical tools such as the mean, standard deviation, and confidence intervals.

The Monte Carlo method fundamentally consists of the following steps: specifying the distributions of input variables and their possible correlations; performing mathematical operations on the sampled inputs to compute the corresponding outputs; repeating the above steps $N$ times to generate output samples; and finally, calculating the mean, variance, confidence intervals, and other statistical properties of the resulting output distribution.

In this context, the characterization of the aforementioned method involves applying the following five steps to approximate the solution of problems involving uncertainties:

1) Model each uncertainty using an appropriate probability density function;
2) Generate pseudo-random values according to the defined probability density functions;
3) Compute the deterministic result by substituting the uncertain variables with the generated values;
4) Repeat steps 2 and 3 until the desired number of samples is obtained (it is noteworthy that increasing the number of samples generally improves the approximation accuracy);
5) Use the collected sample results to obtain consistent estimates of the problem's solution.

### A. Normal Probability Density Function and the Central Limit Theorem

The normal distribution is one of the fundamental tools in probability theory for describing random phenomena. Its significance lies in the fact that many natural processes exhibit characteristics consistent with this distribution, making it a suitable model in a wide range of applications [22].

The probability density function of the normal distribution is expressed as:

$$f(x) = \frac{1}{\sqrt{2\pi}\sigma} \cdot e^{-\left(\frac{1}{2}\right)z^2}, \qquad z = \left(\frac{x - \mu}{\sigma}\right) \tag{12}$$

where $z$ is the standardized variable related to the random variable $x$, $\mu$ is the mean, and $\sigma$ is the standard deviation that quantifies data dispersion.

To illustrate the standard normal distribution, Figure 6 shows the probability density function with shading representing the probability intervals within $\pm 1\sigma$ (68.26%), $\pm 2\sigma$ (95.45%), $\pm 3\sigma$ (99.73%), and $\pm 5\sigma$ (approximately 100%). These shaded regions highlight the cumulative probability for different standard deviations, providing insight into the dispersion of values around the mean ($\mu = 0$) for a normally distributed variable.
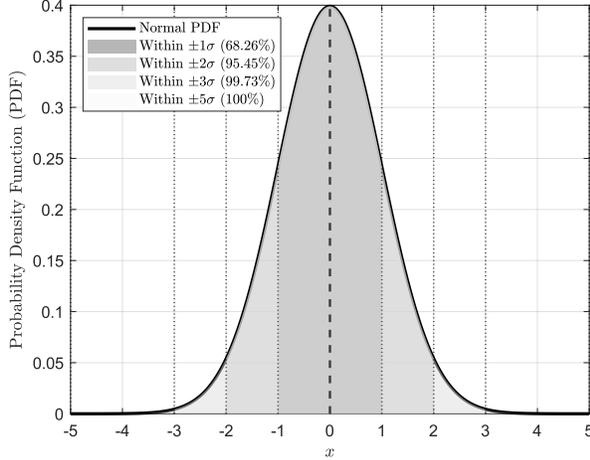
**FIGURE 6. Illustration of the standard normal distribution highlighting the probability intervals within $\pm 1\sigma$ (68.26%), $\pm 2\sigma$ (95.45%), $\pm 3\sigma$ (99.73%), and $\pm 5\sigma$ (approximately 100%).**

In this distribution, the most probable value of the variable $x$ is its mean $\mu$. Moreover, as the value deviates from the mean, its probability of occurrence progressively decreases. This behavior can be quantitatively expressed as:

$$
\begin{aligned}
P(\mu - \sigma < x < \mu + \sigma) &\approx 68.26\% \\
P(\mu - 2\sigma < x < \mu + 2\sigma) &\approx 95.45\% \\
P(\mu - 3\sigma < x < \mu + 3\sigma) &\approx 99.73\% \\
P(\mu - 5\sigma < x < \mu + 5\sigma) &\approx 100\%.
\end{aligned}
\tag{13}
$$

An important property of the normal distribution is that, regardless of the original distribution of a given random variable, for a sufficiently large sample size, the distribution of the sample means tends toward a normal distribution. This phenomenon is justified by the Central Limit Theorem [23], which forms the basis for using Gaussian models in a wide range of engineering applications.

### B. Non-sequential Monte Carlo Simulation

The Non-Sequential Monte Carlo Simulation (NSMCS) approach proposed in this work does not consider the chronological sequence of events within the analyzed system. Instead, NSMCS relies on random sampling of input variables combined with the analysis of five key statistical parameters: the test function, its estimator, the variance of the test function, the variance of the estimator, and the convergence coefficient of the method, denoted by $\beta$.

The test function, denoted by $f_T$, characterizes the behavior of the system under analysis and is formally defined as

$$
f_T : \mathbb{R} \to \mathbb{R}.
\tag{14}
$$

The corresponding estimator, which represents the sample mean of the test function values over $N_S$ samples, is given

by

$$
E(f_T) = \frac{1}{N_S} \sum_{i=1}^{N_S} f_T.
\tag{15}
$$

The variance of the test function, used to quantify the spread of the values around the mean, is computed as

$$
V(f_T) = \frac{\sum_{i=1}^{N_S} \left[ f_T^2 - N_S \cdot (E(f_T))^2 \right]}{N_S - 1}.
\tag{16}
$$

From this, the variance of the estimator $E(f_T)$ can be derived as

$$
V\left(E(f_T)\right) = \frac{V(f_T)}{N_S}.
\tag{17}
$$

Finally, the convergence coefficient $\beta$, which quantifies the numerical stability and convergence behavior of the NSMCS method, is defined as

$$
\beta = \frac{\sqrt{V\left(E(f_T)\right)}}{E(f_T)}.
\tag{18}
$$

In the proposed model for evaluating switching losses in power MOSFETs, the input parameters exhibit stochastic behavior. This uncertainty makes the NSMCS method particularly suitable for estimating switching energy losses while accounting for parameter variability.

Given the probabilistic nature of the variables involved in the switching process, the application of Monte Carlo techniques provides statistically meaningful estimates of energy losses, while also capturing the intrinsic variability of the system.

The next section presents the detailed implementation of the proposed probabilistic methodology, highlighting the modeling assumptions and simulation strategies adopted.

## IV. PROBABILISTIC APPROACH TO SWITCHING LOSS ESTIMATION

The probabilistic approach for switching loss estimation builds upon the foundations discussed in Sections II and III. Figure 7 presents the flowchart that summarizes the implementation of the Monte Carlo-based switching loss estimation strategy.

The following procedure outlines the Monte Carlo-based methodology employed for estimating the switching losses in MOSFETs, as illustrated in Figure 4.

STEP 1: Definition of the maximum number of draws ($N_{S_{\max}}$), the maximum tolerance for the convergence coefficient ($tol$), and initialization of the number of draws to zero ($N_S = 0$);

STEP 2: Obtaining the Probability Density Functions of normal distribution for each of the random variables (MOSFET parameters), followed by drawing values from the generated Gaussian distributions;

STEP 3: Compute switching energies values $E_{on}$, $E_{off}$, and $E_{sw}$ (see Fig. 4);

STEP 4: Update the number of draws ($N_S = N_S + 1$);

STEP 5: Calculate the estimates of the test functions $E(f_T)$ as shown in (19);

$$\widetilde{E}\left[F_T(U)\right] = \frac{1}{N_S} \cdot \sum_{i=1}^{N_S} F_T(U_i) \qquad (19)$$

STEP 6: Compute the variances associated with the test functions and the variances of the estimates, followed by the calculation of the coefficient $\beta$ in (20);

$$\beta = \frac{\sqrt{V\left\{\widetilde{E}\left[F_T(U)\right]\right\}}}{\widetilde{E}\left[F_T(U)\right]} \qquad (20)$$

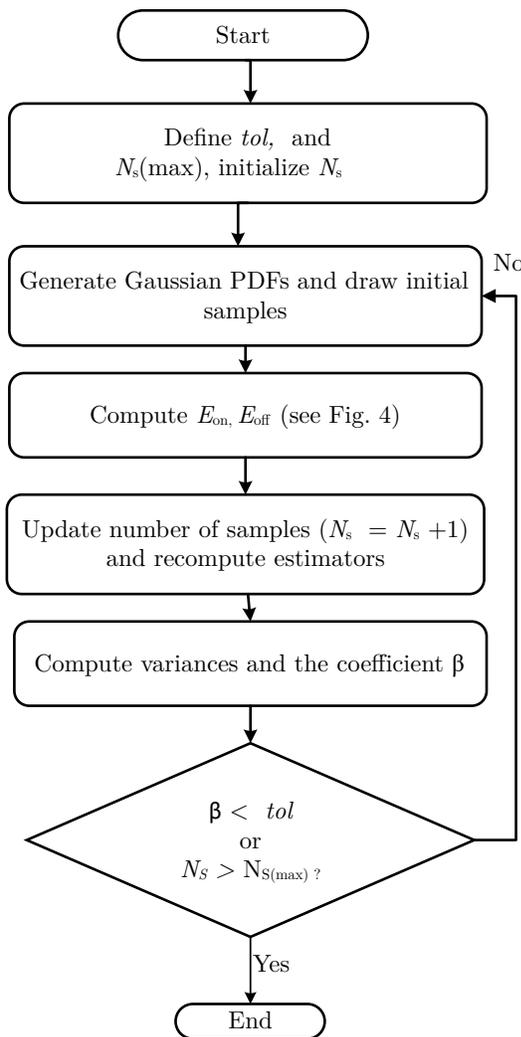STEP 7: Evaluate the convergence of the method according to the condition described in the decision block.



**FIGURE 7. Flowchart representing the Monte Carlo-based switching loss estimation procedure.**



**FIGURE 8. Transconductance curve of the SiC MOSFET SCT3120AL, extracted from the device's datasheet [20].**

**TABLE 2. Mean and standard deviation values for the selected random variables.**

| MOSFET | Variables | Mean | Standard Deviation |
|---|---|---|---|
| | $R_g$ | 28 Ω | 2.8 Ω |
| SCT3120AL | $g_{fs}$ | Function of $i_D$ | Function of $i_D$ |
| | $V_{th}$ | 4.15 V | 1.45 V |
| | $R_g$ | 10.6 | 1.06 |
| IRF840 | $g_{fs}$ | 4.9 | 0.49 |
| | $V_{th}$ | 3 | 1 |

estimates. The total gate resistance $R_g$ was considered with a variation range of 10%, adopting the tolerance range of the external resistor. The choice of the transconductance value was based on a 10% variation around the average value obtained from the curve extracted from the device's datasheet, according to the desired temperature, as illustrated in Figure 8. Finally, the variation of the $V_{th}$ parameter was adopted from the minimum and maximum values presented in the device's datasheet.

Table 2 shows the values of the means and standard deviations associated with each of the random variables for the analyzed devices. These values are important for the generation of the Gaussian PDFs. It is worth noting that the typical value of the threshold voltage was chosen as the mean of the Gaussian PDF.

It is worth emphasizing that the high-level ($V_{dr(on)}$) and low-level ($V_{dr(off)}$) drive voltages were held constant throughout the analysis, in order to isolate the impact of parasitic elements on switching dynamics and energy dissipation.

The random variables were selected based on the sensitivity analysis presented in Section II, which identified the gate resistance, transconductance, and threshold voltage as the most influential parameters affecting switching loss
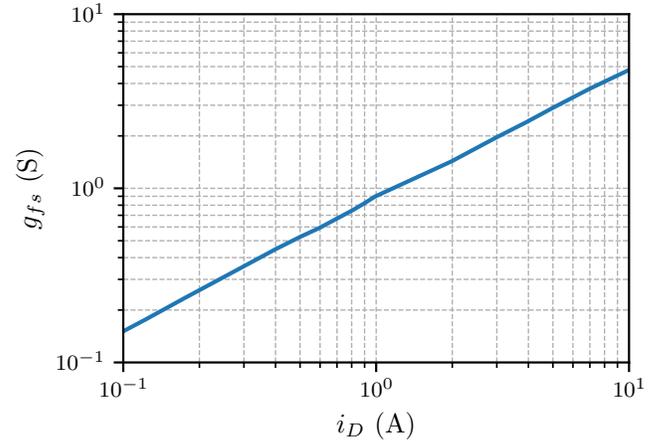
## V. EXPERIMENTAL RESULTS AND DISCUSSION

To experimentally validate the proposed probabilistic approach, a double-pulse test circuit was implemented for switching loss characterization in power MOSFETs. The

Eletrônica de Potência, Rio de Janeiro, v. 30, e202553, 2025.

7

experimental setup is shown in Fig. 9, where key components are clearly identified in Table 3. The printed circuit board includes a dedicated slot for the current probe, eliminating the need for external wiring during measurements. A low-recovery SiC diode ($D_s$) was selected to minimize its impact on switching energy. Voltage waveforms $v_{DS}$ and $v_{GS}$ were captured using 500 MHz passive probes, and the gate-drive circuitry was digitally controlled by a field-programmable gate array (FPGA). To minimize skew effects, a de-skew procedure was applied to the oscilloscope inputs prior to acquisition.
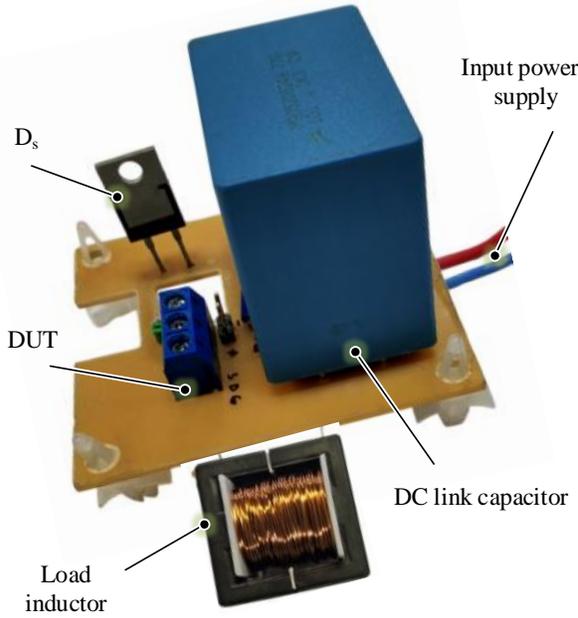


**FIGURE 9. Experimental setup for DPT measurements.**

**TABLE 3. Key Parameters and Parasitic Values of the Double-Pulse Test Circuit.**

| Section | Parameter | Value | Parameter | Value |
|---|---|---|---|---|
| Power circuit | $V_{dd}$ | 100–300 V | $I_{dd}$ | 1–5 A |
| Gate drive circuit | $V_{gg}$ | 18 V | $V_{ggl}$ | 0 V |
| | $R_g$ | 28 Ω (incl. $R_{gint}$ = 18 Ω) | | |
| Diode C3D16065A | $R_d$ (25°C) | 35 mΩ | $V_F$ | 1.5 V |

For the analysis and calculation of switching losses, the signals $v_{DS}$, $v_{GS}$, and $i_D$ acquired by the oscilloscope were stored and subsequently processed using MATLAB routines on a personal computer. A dedicated function was implemented to analyze the collected data for a given set of samples and to extract the relevant information regarding the device energy losses.

As an illustrative example, Fig. 10 presents the waveforms of $i_D$, $v_{GS}$, and $v_{DS}$ for the SCT3120AL MOSFET under a 100 V–4 A operating condition. These waveforms closely resemble the typical behavior presented in Fig. 2, thereby confirming the consistency of the acquired measurements.

Based on these processed signals, both the analytical model and the experimental results corresponding to the dynamics of $v_{DS}$, $v_{GS}$, and $i_D$ during turn-on and turn-off were employed to calculate the dissipated energy over a short time interval. The instantaneous energy, $E_{\text{inst}}(i)$, is obtained through integration of the instantaneous power, $P$, and its evaluation using the trapezoidal approximation over $p$ samples was originally presented in [12] and is adopted in the present work.

In addition to the electrical characterization, the electrothermal behavior was also investigated. All experiments were conducted using a Peltier-based thermal control system, following the procedure described in [13]. This system ensures that the electrical parameters of the device under test remain at the specified temperature conditions, e.g., similar to those defined in the datasheet. Temperature control was achieved using a DC voltage supply in combination with an external monitoring thermocouple, allowing the device junction temperature ($T_{jc}$) to be set at multiple levels. Each measurement was performed under thermal steady-state conditions to guarantee a stable junction temperature during the double-pulse test.

Several MOSFET parameters exhibit temperature dependence. In particular, $R_{ds(on)}$ and $g_{fs}$ present positive temperature coefficients, while $V_{th}$ exhibits a negative coefficient. Although some datasheets provide the variation of these parameters with temperature, this information is not always available and may need to be experimentally determined. Once the temperature-dependent expressions for $g_{fs}(T_{jc})$, $V_{th}(T_{jc})$, and $R_{ds}(on)(T_{jc})$ are obtained, they can be incorporated into the Monte Carlo methodology to account for parameter variability under specific thermal conditions, enabling probabilistic switching-loss estimates at the desired temperature.

The DPT measurements were performed at three bus voltage levels (100 V to 300 V, in 100 V increments) and three load currents (1 A, 2 A, and 5 A). For each operating condition, the proposed method was applied to estimate the switching energy distributions using the SMC-NC algorithm.

Fig. 11 illustrates a representative case, showing the histograms of the switching energies fitted with Gaussian probability density functions, characterized by their mean ($\mu$) and standard deviation ($\sigma$). The corresponding experimental values are superimposed to allow direct comparison and to assess the accuracy of the probabilistic estimates.

The first case analyzed, corresponding to an operating condition of 300V and 1A, is detailed in Fig. 12 and Table 4. Fig. 12 illustrates the estimated probability distributions of the turn-on ($E_{on}$), turn-off ($E_{off}$) and total switching energy ($E_{sw}$) together with the experimental measurements
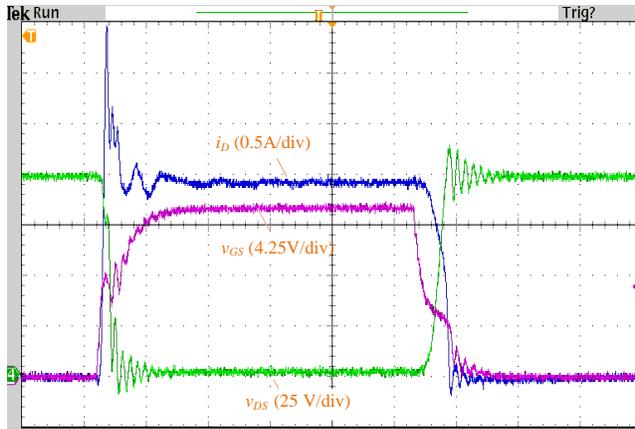
**FIGURE 10. Drain current ($i_D$), gate-to-source voltage ($v_{GS}$), and drain-to-source voltage ($v_{DS}$) waveforms of the SCT3120AL MOSFET at 100 V–4 A.**
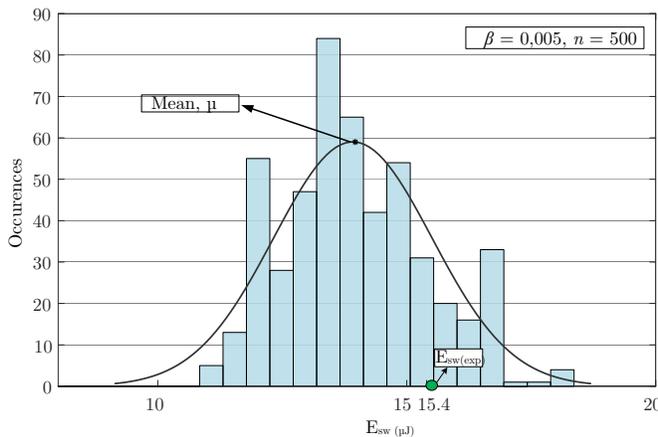


**FIGURE 11. Switching energy estimation using SMC-NC and comparison to experimental result.**

indicated by magenta lines. Table 4 provides a quantitative summary, reporting the mean values and standard deviations of $E_{on}$, $E_{off}$ and $E_{sw}$ under this operating condition. The close agreement between the probabilistic estimates and the experimental results demonstrates the effectiveness and reliability of the proposed Monte Carlo-based approach for switching loss evaluation.

**TABLE 4. Comparison Between Experimental and Probabilistic Estimates at 300 V / 1 A**

| Condition | Method | $E_{on}$ (µJ) | $E_{off}$ (µJ) | $E_{sw}$ (µJ) |
|---|---|---|---|---|
| 300 V / 1 A | Experimental | 18.15 | 5.74 | 23.89 |
| | Probabilistic ($\mu$) | 17.75 | 5.35 | 23.10 |
| | Prob. ($\mu \pm \sigma$) | 17.75 ± 1.25 | 5.35 ± 0.32 | 23.10 ± 1.56 |

To assess the convergence characteristics of the SMC-NC method, Fig. 13 shows the evolution of the estimated switching energy as a function of the number of Monte Carlo
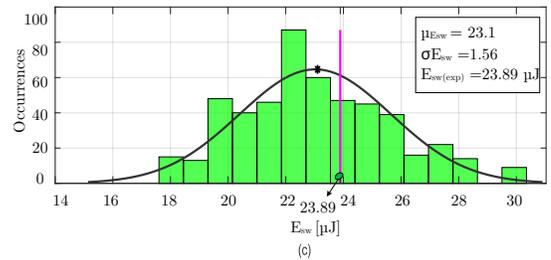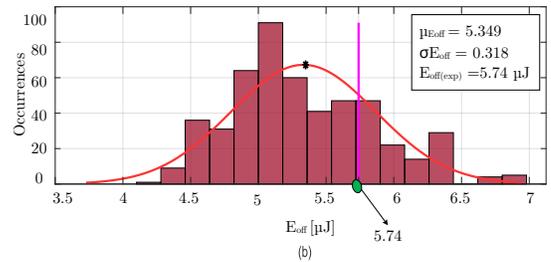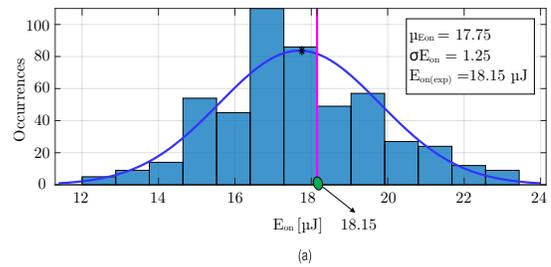


**FIGURE 12. Estimated distributions of $E_{on}$, $E_{off}$, and $E_{sw}$ using the SMC-NC method at 300 V / 1 A.**

samples. Results indicate that approximately 300 samples are sufficient for convergence under this operating condition.
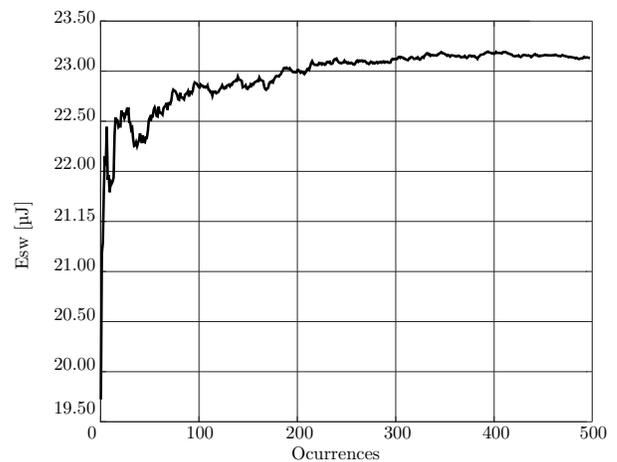


**FIGURE 13. Convergence of switching energy estimation (300 V / 1 A) with Monte Carlo sample size.**

The proposed method was evaluated across 9 operating conditions for the SCT3120AL, covering all voltage and current combinations. The results were compared to two classical estimation methods: the datasheet-based approach

**TABLE 5. Comparison between experimental and estimated switching energies for the SCT3120AL. Values in parentheses denote relative percentage errors.**

| Condition (V-I) | Exp. [$\mu$J] | Proposed [$\mu$J (%)] | [19] [$\mu$J (%)] | [24] [$\mu$J (%)] | [13] [$\mu$J (%)] |
|---|---|---|---|---|---|
| 100–1 | 3.67 | 4.06 (10.6) | 6.96 (89.7) | 3.43 (6.5) | 3.73 (1.63) |
| 100–2 | 8.76 | 8.16 (6.9) | 12.70 (45.0) | 5.61 (36.0) | 7.25 (-17.23) |
| 100–5 | 19.58 | 21.60 (10.3) | 32.30 (65.0) | 14.53 (25.8) | 15.87 (-18.96) |
| 200–1 | 11.30 | 9.62 (14.9) | 17.82 (57.7) | 16.27 (44.0) | 15.41 (36.36) |
| 200–2 | 22.19 | 23.75 (7.0) | 34.85 (57.1) | 23.03 (3.8) | 22.89 (3.17) |
| 200–5 | 52.02 | 47.63 (8.4) | 81.32 (56.3) | 44.39 (14.7) | 41.52 (-20.18) |

**TABLE 6. Comparison between experimental and estimated switching energies for the IRF840. Values in parentheses denote percentage errors.**

| Condition (V–I) | Exp. [$\mu$J] | Proposed [$\mu$J (%)] | [19] [$\mu$J (%)] | [24] [$\mu$J (%)] | [13] [$\mu$J (%)] |
|---|---|---|---|---|---|
| 100–1 | 3.20 | 3.53 (10.31) | 2.51 (−21.56) | 2.61 (−18.44) | 2.81 (−12.19) |
| 100–2 | 4.85 | 5.56 (14.64) | 12.89 (165.77) | 6.56 (35.26) | 6.12 (26.19) |
| 100–6 | 22.10 | 23.28 (5.34) | 38.67 (75.05) | 32.69 (47.88) | 27.34 (23.71) |
| 200–1 | 8.95 | 9.11 (1.79) | 9.54 (6.59) | 11.94 (33.40) | 10.56 (17.99) |
| 200–2 | 13.58 | 17.12 (26.06) | 20.42 (50.34) | 17.70 (30.37) | 17.61 (29.68) |
| 200–6 | 44.19 | 45.29 (2.49) | 82.10 (85.78) | 71.74 (62.31) | 67.57 (52.91) |

by Guo [19], the analytical model by Ahmed [24], and improved method [13]. As presented in Table 5, the probabilistic method outperformed the deterministic approaches in all scenarios. In all 9 analyzed cases, the stochastic method produced results that were consistently closer to the experimentally obtained values. The proposed probabilistic approach is particularly relevant during the pre-design stage of power converters, where engineers must define thermal margins and select components without access to exhaustive experimental data. Unlike deterministic methods, which provide a single nominal value, the Monte Carlo-based methodology delivers a statistical distribution of switching losses, reflecting the variability of key device parameters such as threshold voltage, transconductance, and gate resistance. This information enables designers to anticipate worst-case scenarios and optimize heat sink sizing, gate driver design, and protection strategies with greater confidence. The simulation framework incorporates a discretized capacitance model to account for the nonlinear behavior of $C_{iss}$, $C_{oss}$, and $C_{rss}$ during high $dv/dt$ transitions, ensuring accurate estimation of switching intervals and energy dissipation. Although the method requires a moderate computational effort (approximately 20 minutes per operating point), its ability to capture parameter uncertainty and nonlinear capacitance effects results in predictions that closely match experimental measurements, offering a more robust foundation for early-stage design decisions. Despite its relatively higher computational time when compared to analytical or deterministic methods, it demonstrates a higher degree of accuracy, making it suitable not only for pre-design analysis but also for use in optimization algorithms, particularly in the final design phases (>TRL-6) of power electronic converters for industrial applications.

To extend the proposed probabilistic method, this study also considered a different MOSFET technology, namely the IRF840. For the implementation of the Gaussian distributions, the parameter data described in Table 2 were used. It is important to highlight that, since the MOSFET does not provide a transconductance curve as a function of current variation, only the minimum and maximum limits were considered to generate the Gaussian PDF related to this parameter. A total of six test conditions were analyzed

(two voltage levels and three current levels), as illustrated in Table 6. Once again, it is observed that the probabilistic method yields the closest estimation of the switching losses when compared to the experimental results obtained from the double-pulse test circuit.

It is important to note that analytical methods provide a straightforward mechanism to obtain an initial estimation of switching losses with a very short convergence time—typically less than 1 minute per operating point when executed on a computer equipped with an Intel Core i7 processor (2 GHz, 32 GB RAM). In contrast, the probabilistic method proposed in this work requires an average simulation time of approximately 20 minutes per operating point under the same hardware conditions. This additional computational effort is primarily due to the iterative nature of the Monte Carlo simulation, which involves repeated sampling of key parameters ($V_{th}$, $g_{fs}$, $R_g$) and recalculation of switching intervals and energy losses ($E_{on}, E_{off}, E_{sw}$) until the convergence criterion ($\beta < 0.01$) is satisfied. Despite this higher computational cost, the proposed approach offers a significant advantage in terms of accuracy and robustness, as it captures parameter variability and nonlinear capacitance effects that deterministic methods neglect. Consequently, the method is particularly suitable for design optimization and reliability assessment, where accurate prediction of switching losses is critical.

The results presented in this section demonstrate the effectiveness of the proposed Monte Carlo methodology in capturing the impact of parameter variability on the switching losses of SiC and Si MOSFETs. While the methodology has not been explicitly applied to CoolMOS and GaN devices in this study, its general formulation allows for straightforward extension to these technologies. This is particularly significant, as both superjunction and GaN devices exhibit a strong sensitivity of their switching behavior to device parameter variations, suggesting that the proposed approach can also provide valuable insights for the analysis and design of these families of devices.

## VI. CONCLUSION

This paper proposed a probabilistic switching loss estimation method for Si and SIC MOSFETs based on the Monte Carlo approach, using only datasheet parameters as input.

A sensitivity analysis was performed to identify the most influential parameters contributing to inaccuracies in conventional estimation techniques.

The proposed model integrates a switching loss estimation procedure that accounts for the nonlinear behavior of the intrinsic capacitances of the MOSFETs with a Non-Sequential Monte Carlo Simulation approach, which abstracts from the chronological order of events in the system under analysis. This non-sequential strategy enables a flexible and efficient assessment framework, particularly suitable for systems characterized by time-independent random variables.

To evaluate the accuracy of the proposed methodology, simulations were conducted under various voltage and current conditions. The estimated losses were compared with experimental results obtained from double-pulse test measurements, as well as with three analytical, deterministic computation methods reported in the literature.

The analytical methods presented in [24] and their improved version [13] provide results close to the experimental values. However, they do not exhibit a consistent error pattern: in some cases, the estimated values closely match the expected results, while in others they differ significantly. Although these methods converge relatively quickly, their implementation is complex, requiring the solution of many differential equations and the import of capacitance curves from digitization software. While the method in [19] is straightforward to implement, it tends to overestimate losses and also lacks a consistent error pattern. The proposed Monte Carlo-based approach considers the parametric variation of device parameters according to their sensitivity, using values derived directly from the manufacturer datasheets. This method yields a range of results that more consistently aligns with experimental data, making it suitable for power converter design and optimization. A potential drawback is the relatively long simulation time required for convergence, though such simulations are typically required only to be run a few times, at specific design stages.

Overall, the proposed probabilistic method demonstrated a significant improvement in accuracy compared to conventional deterministic approaches. A key limitation remains the increased computational effort needed for convergence, with simulation times reaching tens of minutes (less than an hour), depending on the complexity of the analyzed case.

## AUTHOR'S CONTRIBUTIONS

**W.J.PAULA:** Conceptualization, Data Curation, Formal Analysis, Investigation, Methodology, Project Administration, Validation, Visualization, Writing – Original Draft, Writing – Review & Editing. **G.M.SOARES:** Conceptualization, Data Curation, Formal Analysis, Investigation, Methodology, Validation, Visualization, Writing – Review & Editing. **P.S.ALMEIDA:** Conceptualization, Data Curation, Formal Analysis, Investigation, Methodology, Validation, Visualization, Writing – Review & Editing. **H.A.C.BRAGA:** Conceptualization, Data Curation, Formal Analysis, Funding Acquisition, Investigation, Methodology, Project Administration, Resources, Supervision, Validation, Visualization.

## DATA AVAILABILITY

The data used in this research is available in the body of the document.

## REFERENCES

[1] W. Taha, F. Juarez-Leon, M. Hefny, A. Jinesh, M. Poulton, B. Bilgin, A. Emadi, "Holistic Design and Development of a 100-kW SiC-Based Six-Phase Traction Inverter for an Electric Vehicle Application", *IEEE Transactions on Transportation Electrification*, vol. 10, no. 2, pp. 4616–4627, 2024, doi:10.1109/TTE.2023.3313511.

[2] Z. Tang, Y. Yang, F. Blaabjerg, "Power electronics: The enabling technology for renewable energy integration", *CSEE Journal of Power and Energy Systems*, vol. 8, no. 1, pp. 39–52, 2022, doi:10.17775/CSEEJPES.2021.02850.

[3] A. Kumar, M. Moradpour, M. Losito, W.-T. Franke, S. Ramasamy, R. Baccoli, G. Gatto, "Wide Band Gap Devices and Their Application in Power Electronics", *Energies*, vol. 15, no. 23, 2022, doi:10.3390/en15239172, URL: https://www.mdpi.com/1996-1073/15/23/9172.

[4] W. J. de Paula, G. H. M. Tavares, D. C. Pereira, G. M. Soares, P. S. Almeida, H. A. C. Braga, "An extensive comparative study of switching losses prediction in power MOSFETs", *in 2018 13th IEEE International Conference on Industry Applications (INDUSCON)*, pp. 105–111, 2018, doi:10.1109/INDUSCON.2018.8627228.

[5] F. Krismer, J. W. Kolar, "Accurate Power Loss Model Derivation of a High-Current Dual Active Bridge Converter for an Automotive Application", *IEEE Transactions on Industrial Electronics*, vol. 57, no. 3, pp. 881–891, 2010, doi:10.1109/TIE.2009.2025284.

[6] H. Wang, F. Wang, J. Zhang, "Power Semiconductor Device Figure of Merit for High-Power-Density Converter Design Applications", *IEEE Transactions on Electron Devices*, vol. 55, no. 1, pp. 466–470, 2008, doi:10.1109/TED.2007.910573.

[7] D. Christen, J. Biela, "Analytical Switching Loss Modeling Based on Datasheet Parameters for MOSFETs in a Half-Bridge", *IEEE Transactions on Power Electronics*, vol. 34, no. 4, pp. 3700–3710, April 2019, doi:10.1109/TPEL.2018.2859974.

[8] J. Chen, H. Peng, Z. Cheng, "Accurate Switching Performance Prediction and Characterization For Wide Range, High Frequency SiC High Voltage Generator", *in IECON 2019 - 45th Annual Conference of the IEEE Industrial Electronics Society*, vol. 1, pp. 5101–5106, 2019, doi:10.1109/IECON.2019.8926743.

[9] C. Qian, Z. Wang, G. Xin, X. Shi, "Datasheet Driven Switching Loss, Turn-ON/OFF Overvoltage, di/dt, and dv/dt Prediction Method for SiC

Eletrônica de Potência, Rio de Janeiro, v. 30, e202553, 2025.

11

MOSFET", *IEEE Transactions on Power Electronics*, vol. 37, no. 8, pp. 9551–9570, 2022, doi:10.1109/TPEL.2022.3152529.

[10] Y. Xu, C. N. M. Ho, A. Ghosh, D. Muthumuni, "A Datasheet-Based Behavioral Model of SiC MOSFET for Power Loss Prediction in Electromagnetic Transient Simulation", *in 2019 IEEE Applied Power Electronics Conference and Exposition (APEC)*, pp. 521–526, 2019, doi:10.1109/APEC.2019.8721881.

[11] D. Cittanti, F. Iannuzzo, E. Hoene, K. Klein, "Role of parasitic capacitances in power MOSFET turn-on switching speed limits: A SiC case study", *in 2017 IEEE Energy Conversion Congress and Exposition (ECCE)*, pp. 1387–1394, 2017, doi:10.1109/ECCE.2017.8095952.

[12] W. J. de Paula, G. H. M. Tavares, G. M. Soares, P. S. Almeida, H. A. C. Braga, "Switching Losses Prediction Methods Oriented to Power MOSFETs: A Review", *IET Power Electronics*, vol. 13, no. 14, pp. 2960–2970, Nov. 2020, doi:10.1049/iet-pel.2019.1003.

[13] W. J. de Paula, G. H. M. Tavares, G. M. Soares, P. S. Almeida, H. A. C. Braga, "An Improved Methodology for Switching Losses Estimation in SiC MOSFETs", *Eletrônica de Potência*, vol. 25, no. 3, pp. 283–292, Sep. 2020.

[14] M. Novak, A. Sangwongwanich, F. Blaabjerg, "Monte Carlo-Based Reliability Estimation Methods for Power Devices in Power Electronics Systems", *IEEE Open Journal of Power Electronics*, vol. 2, pp. 523–534, 2021, doi:10.1109/OJPEL.2021.3116070.

[15] A. Sangwongwanich, F. Blaabjerg, "Monte Carlo Simulation With Incremental Damage for Reliability Assessment of Power Electronics", *IEEE Transactions on Power Electronics*, vol. 36, no. 7, pp. 7366–7371, 2021, doi:10.1109/TPEL.2020.3044438.

[16] J. Callegari, M. Silva, R. de Barros, E. Brito, A. Cupertino, H. Pereira, "Lifetime evaluation of three-phase multifunctional PV inverters with reactive power compensation", *Electric Power Systems Research*, vol. 175, p. 105873, 2019, doi:https://doi.org/10.1016/j.epsr.2019.105873, URL: https://www.sciencedirect.com/science/article/pii/S0378779619301865.

[17] J. Qi, J. Li, H. Feng, J. Shi, M. Fan, C. Jia, D. Zhen, "Reliability Assessment of Wind Power Converter Systems Based on Mission Profiles and Sub Module Life Correlations", *IEEE Access*, vol. 12, pp. 166162–166175, 2024, doi:10.1109/ACCESS.2024.3494876.

[18] J. Brown, "Modeling the switching performance of a MOSFET in the high side of a non-isolated buck converter", *IEEE Transactions on Power Electronics*, vol. 21, no. 1, pp. 3–10, 2006, doi:10.1109/TPEL.2005.861110.

[19] J. Guo, H. Ge, J. Ye, A. Emadi, "Improved Method for MOSFET Voltage Rise-Time and Fall-Time Estimation in Inverter Switching Loss Calculation", *in 2015 IEEE Transportation Electrification Conference and Expo (ITEC)*, pp. 1–6, 2015, doi:10.1109/ITEC.2015.7165780.

[20] ROHM Semiconductor, "SCT3120AL - SiC MOSFET, 650V, 21A, 120m, TO-247N", https://www.rohm.com/products/sic-power-devices/sic-mosfet/sct3120al-product, datasheet, Rev. 005, 2018, URL: https://www.rohm.com/products/sic-power-devices/sic-mosfet/sct3120al-product.

[21] M. G. Pecht, M. Kang, *Uncertainty Representation, Quantification, and Management in Prognostics*, pp. 193–220, 2019, doi:10.1002/9781119515326.ch8.

[22] M. E. Hajiabadi, H. R. Mashhadi, "Analysis of the Probability Distribution of LMP by Central Limit Theorem", *IEEE Transactions on Power Systems*, vol. 28, no. 3, pp. 2862–2871, 2013, doi:10.1109/TPWRS.2013.2252372.

[23] C. L. T. Borges, J. A. S. Dias, "A Model to Represent Correlated Time Series in Reliability Evaluation by Non-Sequential Monte Carlo Simulation", *IEEE Transactions on Power Systems*, vol. 32, no. 2, pp. 1511–1519, 2017, doi:10.1109/TPWRS.2016.2585619.

[24] M. R. Ahmed, R. Todd, A. J. Forsyth, "Predicting SiC MOSFET Behavior Under Hard-Switching, Soft-Switching, and False Turn-On Conditions", *IEEE Transactions on Industrial Electronics*, vol. 64, no. 11, pp. 9001–9011, 2017, doi:10.1109/TIE.2017.2721882.

## BIOGRAPHIES

**Wesley J. de Paula** received his B.Sc. and M.Sc. degrees in Electrical Engineering from the Federal University of São João del-Rei (UFSJ), Brazil, in 2013 and 2015, respectively, and the Ph.D. degree from the Federal University of Juiz de Fora (UFJF) in 2020. Currently, he is an Assistant Professor at the UFSJ. His research interests include high-gain DC–DC converters, characterization of power semiconductor devices, optimization techniques applied to power electronics, electric drives, multilevel converters, and electric and hybrid vehicles. Dr. de Paula serves as a reviewer for several international journals and conferences in the fields of power electronics and electrical engineering.

**Guilherme M. Soares** received the B.Sc., M.Sc., and Ph.D. degrees in Electrical Engineering from the Federal University of Juiz de Fora (UFJF), Juiz de Fora, Brazil, in 2012, 2014, and 2017, respectively. Since 2015, he has been a Professor with the Department of Electrical Engineering at UFJF. His current research interests include power electronic conversion, electric mobility, optimization techniques applied to power electronics, industrial informatics, visible light communication, and the Internet of Things (IoT). Dr. Soares serves as a reviewer for several international journals and conferences in the fields of power electronics and electrical engineering.

**Pedro S. Almeida** received the B.Sc., M.Sc., and Ph.D. degrees in electrical engineering from the Federal University of Juiz de Fora (UFJF), Brazil, in 2010, 2012, and 2014, respectively. Since 2015, he has been a Professor of Electrical Engineering at UFJF, teaching both undergraduate and graduate courses. He has been a researcher with the Modern Lighting Laboratory (NIMO) since 2008, as part of the interinstitutional Power Electronics Systems Research Group (GESEP-UFJF). His main research interests include power electronics, high-efficiency and high-density converters, modular conversion architectures, wide-bandgap semiconductor devices, power factor correction, solid-state lighting, LED drivers, smart grids, electric vehicles, energy storage systems, microcontroller-based digital control, and the modeling, simulation, and control of power conversion systems.

**Henrique A. Braga** Henrique A. C. Braga received the B.S. degree in electrical engineering from the Universidade Federal de Juiz de Fora (UFJF), Brazil, in 1982 and the Dr. Eng. degree from the Universidade Federal de Santa Catarina, Florianopolis, Brazil, in 1996. Since 1985, he has been teaching Basic Electronics and Power Electronics at the Universidade Federal de Juiz de Fora, in undergraduate and graduate levels. From 2005 to 2006 he was enrolled in a post-doctoral cooperation at Universidad de Oviedo, Gijon, Asturias, Spain. Dr. H. Braga is the author or co-author of more than 200 scientific papers in peer-reviewed technical conferences and journals. He also co-authored six book chapters. Prof. H. Braga is IEEE Life Senior Member and served the Institute as the Brazil Council Chairman, from 2010 to 2011. Prof. Braga chaired the Brazilian Power Electronics Society (Sobraep) from 2014-2015 and was the editor-in-chief of the Brazilian Journal of Power Electronics (now Open Journal of Power Electronics) from 2012 to 2013. Prof. Braga's research interests are mainly related to the Power Electronics field, especially in electronic lighting systems and renewable resources applications. Since 2022 he has been the Dean of Engineering School at Universidade Federal de Juiz de Fora, an administrative position to be developed up to 2026.